8516–8528 *Nucleic Acids Research, 2015, Vol. 43, No. 17* *Published online 3 August 2015*
doi: 10.1093/nar/gkv779

Genome-wide analysis of YB-1-RNA interactions reveals a novel role of YB-1 in miRNA processing in glioblastoma multiforme

Shuai-Lai Wu[1], Xing Fu[2,†], Jinyan Huang[3,†], Ting-Ting Jia[1], Feng-Yang Zong[1], Shi-Rong Mu[1], Hong Zhu[1], Yong Yan[4], Shuwei Qiu[5], Qun Wu[6], Wei Yan[6], Ying Peng[5], Juxiang Chen[4] and Jingyi Hui[1,*]

[1]State Key Laboratory of Molecular Biology, Institute of Biochemistry and Cell Biology, Shanghai Institutes for Biological Sciences, Chinese Academy of Sciences, Shanghai 200031, China, [2]Shanghai Center for Plant Stress Biology, Shanghai Institutes for Biological Sciences, Chinese Academy of Sciences, Shanghai 201602, China, [3]State Key Laboratory of Medical Genomics, Shanghai Institute of Hematology, Rui Jin Hospital Affiliated with Shanghai Jiao Tong University School of Medicine, Shanghai 200025, China, [4]Department of Neurosurgery, Shanghai Institute of Neurosurgery, Chang Zheng Hospital, Second Military Medical University, Shanghai 200003, China, [5]Department of Neurology, The Sun Yat-sen Memorial Hospital, Sun Yat-sen University, Guangzhou 510120, China and [6]Department of Neurosurgery, The Second Affiliated Hospital, School of Medicine, Zhejiang University, Hangzhou 310009, China

Received June 09, 2015; Revised July 16, 2015; Accepted July 21, 2015

ABSTRACT

Altered miRNA expression is believed to play a crucial role in a variety of human cancers; however, the mechanisms leading to the dysregulation of miRNA expression remain elusive. In this study, we report that the human Y box-binding protein (YB-1), a major mRNA packaging protein, is a novel modulator of miRNA processing in glioblastoma multiforme (GBM). Using individual nucleotide-resolution crosslinking immunoprecipitation coupled to deep sequencing (iCLIP-seq), we performed the first genome-wide analysis of the *in vivo* YB-1-RNA interactions and found that YB-1 preferentially recognizes a UYAUC consensus motif and binds to the majority of coding gene transcripts including pre-mRNAs and mature mRNAs. Remarkably, our data show that YB-1 also binds extensively to the terminal loop region of pri-/pre-miR-29b-2 and regulates the biogenesis of miR-29b-2 by blocking the recruitment of microprocessor and Dicer to its precursors. Furthermore, we show that down-regulation of miR-29b by YB-1, which is up-regulated in GBM, is important for cell proliferation. Together, our findings reveal a novel function of YB-1 in regulating non-coding RNA expression, which has important implications in tumorigenesis.

INTRODUCTION

MiRNAs are a class of small non-coding RNA molecules, typically ∼22 nt in length, which in most cases negatively regulate target gene expression (1). The biogenesis of miRNA takes place mainly via a two-step processing pathway. In the nucleus, the long primary transcripts of miRNAs (pri-miRNAs) are transcribed by RNA polymerase II (polII) and processed by the microprocessor complex composed of an RNaseIII enzyme, Drosha, and its binding partner DGCR8, generating the miRNA precursors (pre-miRNAs) with a hairpin structure of 60–70 nt (2–5). Exprotin5 subsequently recognizes the characteristic 3′ overhang structure of pre-miRNA hairpin, and exports pre-miRNAs into the cytoplasm (6). In the cytoplasm, another RNaseIII enzyme, Dicer, further cleaves pre-miRNAs into miRNA duplexes of ∼22 nt (7). One strand of the duplex is loaded by Argonaute to form the active RNA-induced silencing complex (RISC) (8). The mature miRNA guides RISC to target mRNAs by base-pairing, leading to gene repression through mRNA degradation and/or translational repression. Like protein coding genes, the expression patterns of miRNA genes are also subject to temporal and spatial regulation in different types of tissues and cells. MiRNAs are crucial modulators in normal development, differentiation, and cellular homeostasis. Changes in the expression of miRNAs have been associated with a variety range of pathological processes including tumorigenesis (9). Although several RNA-binding proteins have been shown to regulate miRNA expression at post-transcriptional level

*To whom correspondence should be addressed. Tel: +86 21 54921354; Fax: +86 21 54921011; Email: jyhui@sibcb.ac.cn
†The authors wish it to be known that, in their opinion, X.F. and J.H. contributed equally to this work.

(10–15), the mechanisms by which RNA-binding proteins control miRNA expression in cancers remain elusive.

The Y box-binding protein 1 (YB-1) is a member of DNA/RNA binding family of proteins with an evolutionarily conserved cold shock domain (CSD). At molecular level, YB-1 is involved in the regulation of DNA replication and repair, mRNA transcription, splicing, stability and translation (16,17). A number of studies have reported that the elevated level of YB-1 protein is associated with cancer progression and poor prognosis in a variety of cancers including GBM (18,19). In a transgenic mouse model, YB-1 promotes breast tumor formation with a 100% penetrance, indicating that YB-1 has strong oncogenic potential (20). The oncogenic effects of YB-1 characterized so far have been attributed to its roles in the regulation of transcription and translation of several genes that are involved in cell growth, malignant transformation, drug resistance and epithelial-mesenchymal transition (EMT) (21–26). However, the key targets of YB-1 at post-transcriptional level during tumorigenesis are largely unknown.

YB-1 contains an N-terminal alanine/proline-rich (A/P) domain, a central CSD and a C-terminal domain (CTD) carrying alternating clusters of positively and negatively charged amino acid residues. The CSD of YB-1 contains consensus sequences of ribonucleopreotein particle domain-1 and -2 (RNP-1 and RNP-2), which are responsible for the specific and non-specific interaction with RNA, while the A/P domain and the CTD may stabilize its RNA binding (27–29). The CTD can also bind RNA non-specifically and mediate interactions with other protein partners (30–32). It has long been recognized that YB-1 is a major component of mRNP and binds mRNAs non-specifically with high affinity (33,34), although it is capable of interacting some of its targets with sequence preference (35,36). However, to what extent YB-1 binds RNA specifically *in vivo* has not been characterized.

Here, we report the first global study of YB-1-RNA interactions by performing iCLIP-seq (37) in a glioblastoma cell line. Our data demonstrate that YB-1 binding sites are extensively enriched in the protein-coding genes with a consensus binding motif UYAUC. Remarkably, we identify YB-1 as a critical modulator of miRNA dysregulation in GBM and unravel a novel role of YB-1 in the regulation of miRNA processing during tumorigenesis.

MATERIALS AND METHODS

iCLIP-seq analysis

The iCLIP assay was carried out as described (37). Briefly, one 10 cm dish of U251-MG cells were irradiated with UV light at 150 mJ/cm^2. After cell lysis, RNAs were partially fragmented using 10 μl high (1:50) or low (1:5000) dilutions of 5 μg/μl RNase A (QIAGEN) followed by immunoprecipitation with 10 μg anti-YB-1 antibody (Sigma) immobilized on protein A Dynabeads (Life Technologies). RNAs were then ligated at 3′ ends to a DNA adapter and radioactively labeled by T4 polynucleotide kinase (Fermentas), and the protein–RNA complex was transferred to a nitrocellulose membrane. For iCLIP cDNA library preparation, RNAs were purified and reverse-transcribed with a primer containing barcode. The resulting cDNAs were purified by PAGE, circularized by single-stranded DNA ligase (Epicentre), linearized by restriction enzyme cleavage, and amplified by PCR.

The iCLIP cDNA library was processed on an Illumina HiSeq 2000 sequencer. Mapping of sequence reads was performed against the human genome (version Hg19/NCBI37) allowing one mismatch and single hits using Bowtie (38). Identification of clustered crosslink sites was performed as described (37,39). To analyze the enriched motif, the 21 nt-long sequences were extracted by extending 10 nt from the crosslink sites in both directions. The *z*-score for each hexamer in the 21 nt region was calculated relative to control sequences randomly selected from similar background. The top 20 motifs with the highest z-scores were performed the multiple sequence alignment using CLUSTALW. The output file was submitted to the WebLogo3 to generate the sequence logo. To investigate whether YB-1 binding sites are enriched on any pre-miRNAs, the iCLIP cDNA counts were normalized to the expression levels of individual mature miRNA detected by small RNA-seq analysis.

Data access

The iCLIP cDNA counts for YB-1 crosslink sites could be viewed using IGV tool (www.broadinstitute.org/igv/) by uploading a tdf file from www.sibcb.ac.cn/hui.asp.

Small RNA-seq analysis

The short reads of small RNA-seq data were processed by cutadapt (40) to trim the adaptor sequences, and aligned to human genome (hg19) by bowtie (38) using the parameter of '-v1 –best –strata –k11 –m10'. We used the BEDTools (41) and the GFF3 file downloaded from miRBase (42) to quantify the aligned reads on each miRNA. The expression values of miRNAs were normalized by the total number of aligned reads in each library.

Cell culture and RNAi

The human U251-MG and HEK 293T cells were grown in Dulbecco's modified Eagle's medium supplemented with 10% fetal bovine serum. Cells were transfected with control siRNA (5′- ATCCCGUACGCGGAAUACUdTdT-3′) and YB-1 siRNA (5′-GGUCAUCGCAACGAAGGUUdTdT-3′). Stable cell lines expressing control- or YB-1-specific shRNAs were established as previously described using lentivirus system (43).

Plasmid construction

To clone pri-miRNA plasmids, PCR fragments containing pri-miR-24–1, pri-miR-29b-2, pri-miR-29b-1-29a, pri-miR-29b-2-29c were amplified from U251-MG genomic DNA using cloning primers listed in the supplementary table and inserted into pcDNA3 vector (Invitrogen). Substitution of AUC in the wildtype loop of miR-29b-2 with UAG was made by a two-step PCR using primers listed in the supplementary table. To clone control and YB-1 shRNA

expression constructs, DNA fragments encoding control and YB-1 shRNAs were annealed and inserted into a modified lentivirus vector containing eGFP coding sequence under the control of CMV promoter. To clone the YB-1 shRNA-resistant construct, nucleotides GTC ATC GCA ACG AAG GTT encoding amino acids 54–59 were mutated to GTT ATT GCC ACC AAA GTC by PCR. Then, the entire YB-1 coding sequence was fused to the 3′ end of eGFP coding sequence.

Western blotting

To extract protein samples from patient tissues, normal and tumor tissues were homogenized in RIPA buffer containing 50 mM Tris–Cl pH 7.4, 150 mM NaCl, 1% NP-40, 1 mM EDTA-free protease inhibitor cocktail (Roche) plus 1.5 mM phenylmethylsulfonyl fluoride (PMSF). Lysates were collected following the removal of insoluble material from tissue extracts by centrifugation at 14 000 rpm for 20 min at 4°C. Protein lysates were separated by SDS-PAGE followed by gel transfer to a nitrocellulose membrane (Bio-Rad). The membranes were incubated first with the primary antibodies, and then with secondary antibodies coupled to horseradish peroxidase (HRP). Band signals were detected with an enhanced chemiluminescence (ECL) system (Thermo Scientific) and visualized by image analyzer (Fujifilm). The primary antibodies used for this study are anti-GAPDH (Kang Cheng Bio-tech, China), anti-γ-tubulin (Sigma), anti-FLAG (Sigma) and anti-YB-1 (Sigma). The HRP-conjugated secondary antibodies anti-mouse IgG and anti-rabbit IgG were purchased from Promega.

Gel shift assay

^{32}P labeled *in vitro* transcribed RNAs (80 fmol) of about 2000 cpm were mixed with 0.4 μl 80 mM $MgCl_2$, 1.0 μl 10 μg/μl tRNA, 0.4 μl RNaseIn (40 U/μl, Fermentas), 1.2 μl native loading buffer (60% glycerol, 0.1% bromophenol blue, 0.1% xylene cyanol), and 6 μl His-YB1 with dosage gradient. After 15 min of incubation at 37°C, the 10 μl solution was loaded onto a 5% native gel followed by autoradiography.

Northern blotting

Total RNAs (5–10 μg) were resolved on a 15% denaturing polyacrylamide gel and transferred to positively charged nylon membrane (Roche) by semi-dry transfer apparatus (Bio-Rad) and UV-crosslinked at 125 mJ/cm^2. Oligonucleotides complementary to miRNA were end-labeled by T4 polynucleotide kinase (Fermentas) and used as probes. Hybridization was carried out at 58°C using Perfect Hybridization Solution (TOYOBO). The membrane was washed by buffer (2X SSC, 0.1 SDS) pre-warmed at 58°C and then exposed to a phosphor image plate (Fujifilm). For re-hybridization, the membrane was striped by boiling in buffer containing 0.1% SDS at 85°C for 15 min.

Real-time quantitative reverse-transcription polymerase chain reaction (RT-qPCR)

Total RNA was prepared with TRIzol reagent (Life Technologies) according to the manufacturer's protocol. RNA (2 μg) was treated with DNaseI (Fermentas) and then used for first-strand cDNA synthesis with SuperScript III (Life Technologies). MiRNAs were detected by a stem-loop reverse primer according to previously described protocol (44), and the sequences of oligonucleotides were listed in the supplementary table. *P*-values were calculated by paired one-tailed t-test. The expression levels of miR-29b in different tissues were normalized to that in N1 sample.

RNA immunoprecipitation (RIP)

HEK 293T cells were transfected with pri-miRNA and YB-1 expression plasmids using calcium phosphate methods. 48 h after transfection, cells were irradiated with UV light at 150 J/cm^2, harvested, and lysed in iCLIP lysis buffer. After centrifugation at 20 000g for 10 min, the supernatant was incubated with 10 μl anti-FLAG M2 magnetic beads (Sigma) for 2 h at 4°C. After washing, the bound RNAs were isolated using TRIzol reagent (Invitrogen) followed by RT-qPCR or Northern blotting analysis.

In vitro transcription and processing of pri-miRNA

^{32}P-labeled pri-miRNAs were *in vitro* transcribed by T7 RNA polymerase (Fermentas) using XbaI-linerarized pcDNA3-pri-miRNA plasmids as templates. *In vitro* processing of pri-miRNAs was carried out as previously described with some modifications (10). Briefly, reactions were setup in 25 μl volume containing 15 μl of HeLa nuclear extract (Cil Biotech), 6.4 mM $MgCl_2$, 0.8 U/μl RNaseIn (Fermentas) and labeled RNAs of about 100 000 cpm. After incubation at 37°C for 90 min, total RNAs in the reaction were extracted with phenol and resolved on a 10% urea polyacrylamide gel.

In vitro transcription and processing of pre-miRNA

Pre-miRNAs were prepared using a 5′ hammerhead ribozyme as described previously (45). Briefly, DNA fragment containing 5′ hammerhead ribozyme and pre-miRNA sequences were amplified by PCR using primers listed in the supplementary table. *In vitro* transcribed RNAs were gel-purified using a 8% denature polyacrylamide gel to remove uncleaved RNAs and ribozyme RNAs. Then, the recovered RNAs were fractionated again on a 20% denature polyacrylamide gel to purify the homogeneous pre-miRNAs followed by phosphorylation at 5′ ends by T4 polynucleotide kinase (Fermentas). ^{32}P-labeled pre-miRNAs of about 100 000 cpm were incubated with recombinant His-YB-1 protein and FLAG-tagged Dicer in reaction buffer containing 25 mM Tris–Cl pH 7.5, 125 mM NaCl, 6.4 mM $MgCl_2$, 2 mM EDTA and 5% glycerol. Total RNAs were extracted by phenol and resolved on a 15% urea polyacrylamide gel. The purified and kinased ^{32}P-labeled pre-miRNA substrates were treated with alkaline to serve as RNA marker.

In vitro RNA pulldown assay

FLAG-tagged DGCR8 or Dicer immobilized on beads was incubated with ^{32}P-labeled pri-miRNA or pre-miRNA in the presence of recombinant His-YB-1 protein. To block

Dicer enzyme activity, $MgCl_2$ was omitted in the buffer. After incubation at 37°C for 30 min, the bound RNAs were washed, extracted by phenol, and resolved on a 10% or 15% denaturing polyacrylamide gel.

GBM patient tissues

All GBM normal and tumor tissues were collected from patients in Chang Zheng Hospital, Shanghai, China with approval from the Institute Research Ethics Committee.

Expression correlation analysis

The expression data of miR-29b and YB-1 mRNA were downloaded from the Cancer Genome Atlas data portal (July 2012) (46). The expression data for miR-29b and YB-1 mRNA are available for 472 GBM patients. The Pearson's correlation coefficient and significance *P*-value between miR-29b and YB-1 mRNA expression values were calculated using Matlab.

MTT cell proliferation assay

MTT assay was performed as previously described (43).

Protein purification

GST-tagged and His-tagged YB-1 proteins were purified from *Escherichia coli* strain BL21 DE3 cells as previously described (32). To prepare FLAG-tagged DGCR8 and Dicer, pCK-FLAG-DGCR8 and pCK-FLAG-Dicer plasmids kindly provided by Dr Narry Kim were transfected into HEK 293T cells. After cell lysis, immuno-purification was carried out using anti-FLAG M2 beads as previously described (47). To remove co-purified proteins with DGCR8, the beads were washed extensively as previously described (3).

RESULTS

Genome-wide mapping of YB-1-RNA interactions by iCLIP-seq

To search for *in vivo* RNA targets of YB-1, we performed iCLIP experiments with U251-MG glioblastoma cells. After UV irradiation and RNase partial digestion, specific YB-1–RNA complex was immunoprecipitated with an antibody against YB-1 (Figure 1A). RNAs in the complex were recovered for cDNA library preparation followed by deep sequencing. In total, 108 million iCLIP tags were generated with YB-1-specific antibody. In comparison, only 215 054 tags were obtained with a control antibody. Following removal of PCR amplification artifacts, 61.9 million unique cDNA reads corresponding to 17.2 million YB-1 crosslink sites were aligned to the human genome by allowing one nucleotide mismatch and single genomic hits (YB-1 crosslink sites could be viewed by uploading a tdf file from www.sibcb.ac.cn/hui.asp into IGV tool (www.broadinstitute.org/igv/)). Using additional filtering algorithms, we identified 926 511 clustered crosslink sites, representing the most promising YB-1 binding sites. The crosslink sites grouped in clusters are highly reproducible among three independent replicates (Figure 1B).

Consistent with the notion that YB-1 is a major mRNA packaging protein, 96.3% of cDNA reads were uniquely mapped to the annotated coding genes, with 51% in 3′-UTR and 36% in coding sequence (Figure 1C). The clustered crosslink sites are dispersed in 15 084 transcribed coding genes. We detected 4 292 537 and 1 136 536 cDNA reads that overlap with exon–exon and exon–intron junctions, respectively, indicating that YB-1 binds both pre-mRNA and spliced mRNA (Figure 1D). Genomic annotation of the cDNA reads also shows that 2% of cDNA reads are derived from intergenic regions and non-coding RNA loci, respectively (Figure 1C). In non-coding RNA category, miRNA hairpin loci made up 0.03% of total cDNA reads.

In vivo RNA binding specificity of YB-1

To define the RNA binding specificity of YB-1 *in vivo*, we extracted the 21 nt sequence tags containing 10 nt upstream and 10 nt downstream sequences surrounding the crosslink sites to search for enriched hexamer motifs using randomly selected sequences as background. Based on *z*-scores, we identified the overrepresented hexamers and deduced the YB-1 binding consensus as UYAUC (Figure 1E). Using SELEX approach, we previously identified that YB-1 binds to RNAs containing a CAU/CC motif with high affinity *in vitro*. Mutational analysis has shown that the first C in this motif is tolerated, since YB-1 bound to a mutant RNA with the first C substituted with G as efficiently as the wildtype RNA (32). Thus, the *in vivo* binding consensus identified by iCLIP in this study closely resembles the *in vitro* SELEX motif that we determined previously. In addition, we found that at least 17.8% of tags (containing 20 nt upstream and 20 nt downstream sequence flanking the crosslink site) contain YB-1 binding consensus UYAUC, indicating that YB-1 binds to a significant fraction of RNAs with sequence specificity, although it is known as an abundant protein which packs mRNA non-specifically.

YB-1 binding sites are enriched in the terminal loop of miR-29b-2

Since YB-1 binding sites were detected in the stem-loop region of miRNAs, we investigated whether YB-1 binding sites are enriched on any miRNA precursors of YB-1-regulated miRNAs. We carried out small RNA-seq with total RNAs purified from control- or YB-1- knockdown U251-MG cells. Small RNA-seq detected 32 miRNAs up- or down-regulated in response to YB-1 knockdown (Supplementary Figure S1A). MiR-221 and miR-222 are two miRNAs that have been extensively studied in glioma. They are frequently up-regulated in GBM and play crucial roles in promoting glioma cell proliferation, survival, and invasion (48–51). MiR-221/222 cluster is located on the chromosome X, and they share the same miRNA seed sequence. We found that both the mature miR-221/222 and pri-miR-221/222 transcript decreased upon knockdown of YB-1, suggesting YB-1 up-regulates miR-221/222 production through regulating the expression of their host genes (Supplementary Figure S1B–D). Among the YB-1-regulated

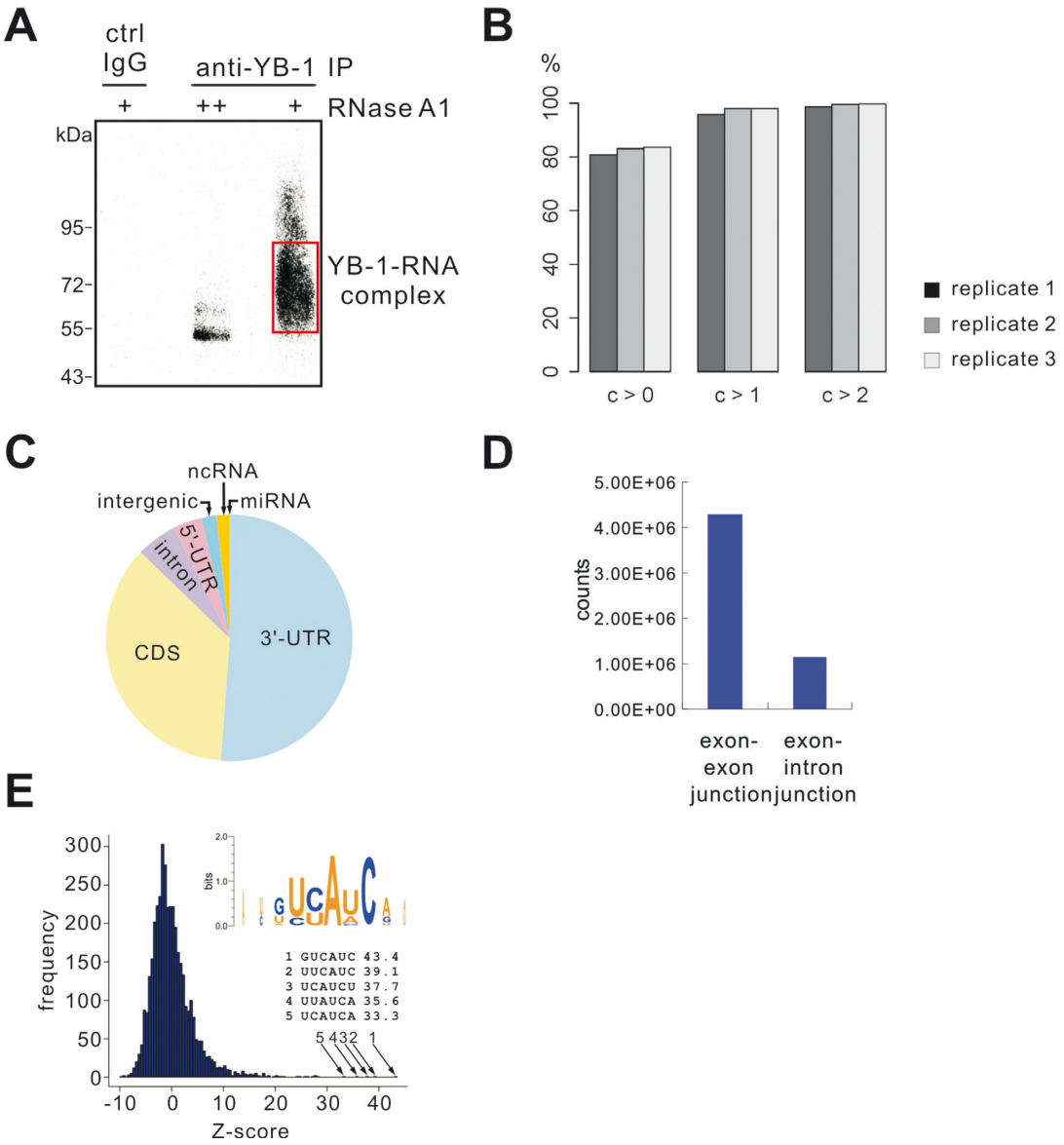

Figure 1. Genome-wide mapping of *in vivo* YB-1 binding sites by iCLIP-seq. (**A**) Phosphorimage of YB-1-RNA complex fractionated by SDS-PAGE. Cell extracts were treated with two concentrations of RNase A1 (high ++; low +) followed by immunoprecipitation with a control or YB-1-specific antibody. RNAs crosslinked to YB-1 were ^{32}P-labeled, and RNA-protein adducts above the position of YB-1 (marked by a red box) were purified for iCLIP library preparation. (**B**) Reproducibility of YB-1 iCLIP crosslink sites. The crosslink sites in one replicate experiment are grouped according to their cDNA count (C>0, all sites taken; C>1, minimal cDNA count of 2; C>2, minimal cDNA count of 3). The bars in the figure represent the average percentage of crosslink sites in one replicate that are present in at least one of the two other replicates. (**C**) Genomic distribution of cDNAs for YB-1 clustered crosslink sites. (**D**) The number of YB-1 iCLIP tags mapped to exon-exon and exon-intron junctions. (**E**) Histogram of *z*-scores for hexamers in tags containing 10 nt upstream and 10 nt downstream sequences surrounding the crosslink sites. Inserts are the deduced consensus based on top 20 hexamers and the top 5 overrepresented hexamers.

miRNAs, YB-1 crosslink sites were detected in the hairpin structure of 4 miRNAs (cDNA counts >10). After iCLIP reads were normalized to the expression levels of individual mature miRNA, we found that YB-1 iCLIP cDNAs are enriched in the terminal loop region of miR-29b-2 (Figure 2A).

To validate the iCLIP-seq results, we prepared *in vitro* transcribed pri-miR-29b-2 RNAs containing the wildtype or the mutant terminal loop sequence. In the mutant RNA, the YB-1 binding site in the loop sequence was substituted as shown in Figure 2B. Gel shift analysis showed that YB-1 bound to the wildtype pri-miR-29b-2 with much higher affinity than the mutant one (Figure 2C). Together, these data indicate that YB-1 binds specifically to the terminal loop of miR-29b-2.

YB-1 suppresses miR-29b-2 maturation by binding to the loop sequence of miR-29b-2

To determine whether YB-1 binding to miRNA loop sequence regulates miRNA expression, we first did Northern blot analysis to test whether YB-1 controls the expres-

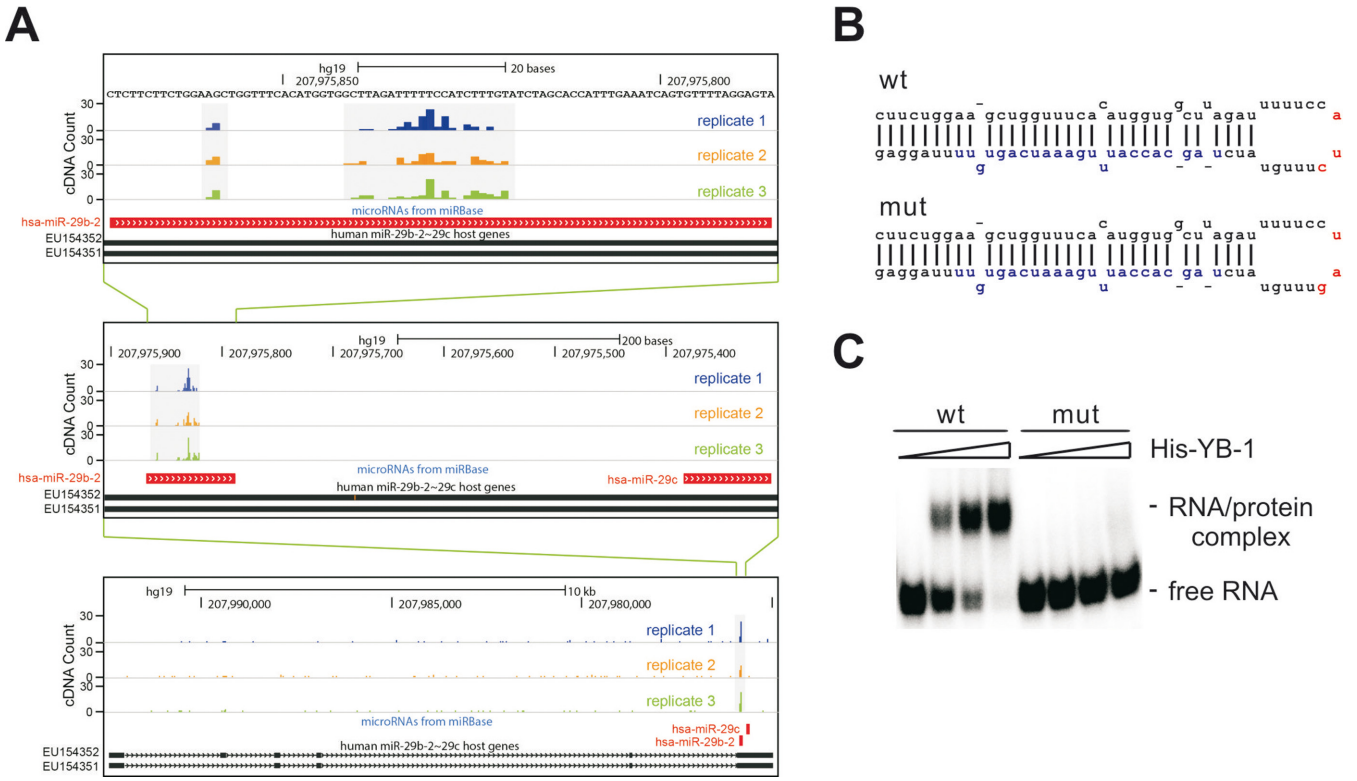

Figure 2. YB-1 binding sites are enriched in the terminal loop region of miR-29b-2. (**A**) iCLIP raw cDNA counts for YB-1 crosslink sites in miR-29b-2/-29c loci. Genomic sequence is shown above the cDNA counts from 3 replicates. (**B**) Schematic representation of the wildtype and the mutant sequences of miR-29b-2 hairpin. (**C**) Gel shift analysis of YB-1 binding to miR-29b-2. ^{32}P-labeled wildtype and mutant pri-miR-29b-2 substrates were incubated with 0, 10, 20 and 40-fold molar excess of recombinant His-YB-1. RNA-protein complexes were fractionated on a 5% native polyacrylamide gel and visualized by autoradiography.

sion level of miR-29b-2. As shown in Figure 3A, knockdown of YB-1 led to an increase in endogenous miR-29b expression, while re-introduction of an shRNA-resistant YB-1 construct reversed the effect. The miR-29b RNA can be expressed from two related miRNA clusters located in two genomic loci, miR-29b-1/miR-29a on chromosome 7 and miR-29b-2/miR-29c on chromosome 1 (52). The mature sequences of miR-29b-1 and miR-29b-2 are identical. To determine whether YB-1 inhibits the expression of miR-29b-1, miR-29b-2 or both, we transfected YB-1 expression construct together with pri-miRNA plasmids derived from two miR-29b loci, separately. Notably, overexpression of YB-1 inhibited the maturation of miR-29b-2, but had no effect on miR-29b-1 (Supplementary Figure S2). Real-time RT-qPCR analyses showed that knockdown of YB-1 did not affect the expression of primary transcripts for miR-29b-1 and miR-29b-2, suggesting that YB-1 regulates the expression of miR-29b by controlling miR-29b-2 production at the post-transcriptional level (Figure 3A).

Next, we tested whether YB-1 inhibited the maturation of miR-29b-2 through binding to the loop sequence of miR-29b-2. We transfected YB-1 expression construct together with pri-miR-29b-2 expression plasmids carrying wildtype or mutant loop sequence into HEK 293T cells. Northern blotting results indicate that YB-1 specifically inhibited the production of mature miR-29b-2 from wildtype pri-miR-29b-2, but not that from mutant pri-miR-29b-2 (Figure 3B). In addition, we observed that overexpression of YB-1 resulted an accumulation of pre-miR-29b-2 generated from wildtype pri-miR-29b-2, suggesting that YB-1 may inhibit the Dicer cleavage of pre-miR-29b-2. These data demonstrate that YB-1 represses miR-29b-2 processing through specific binding to the loop sequence of miR-29b-2.

To identify at which processing step YB-1 recognizes the loop sequence of miR-29b-2, we performed RNA immunoprecipitation (RIP) experiments by pulling down YB-1-bound RNAs in cells expressing FLAG-tagged YB-1 and wildtype or mutant pri-miR-29b-2. The YB-bound pri-miR-29b-2 RNAs were detected by real-time RT-qPCR. We detected YB-1 binding to both wildtype and mutant pri-miR-29b-2; however, YB-1 bound more efficiently to wildtype pri-miR-29b-2 than to the mutant one (Figure 3C). Northern blotting results showed that YB-1 bound specifically to the wildtype pre-miR-29b-2 via the identified YB-1 binding site in the loop region of pre-miR-29b-2 (Figure 3D). Taken together, these data indicate that YB-1 recognizes its binding site in the loop of both primary and precursor of miR-29b-2.

YB-1 represses miR-29b processing at both Drosha and Dicer cleavage steps

The role of YB-1 in suppressing miR-29b-2 maturation and the binding of YB-1 to the loop regions of both pri- and pre-miR-29b-2 led us to hypothesize that YB-1 regulates

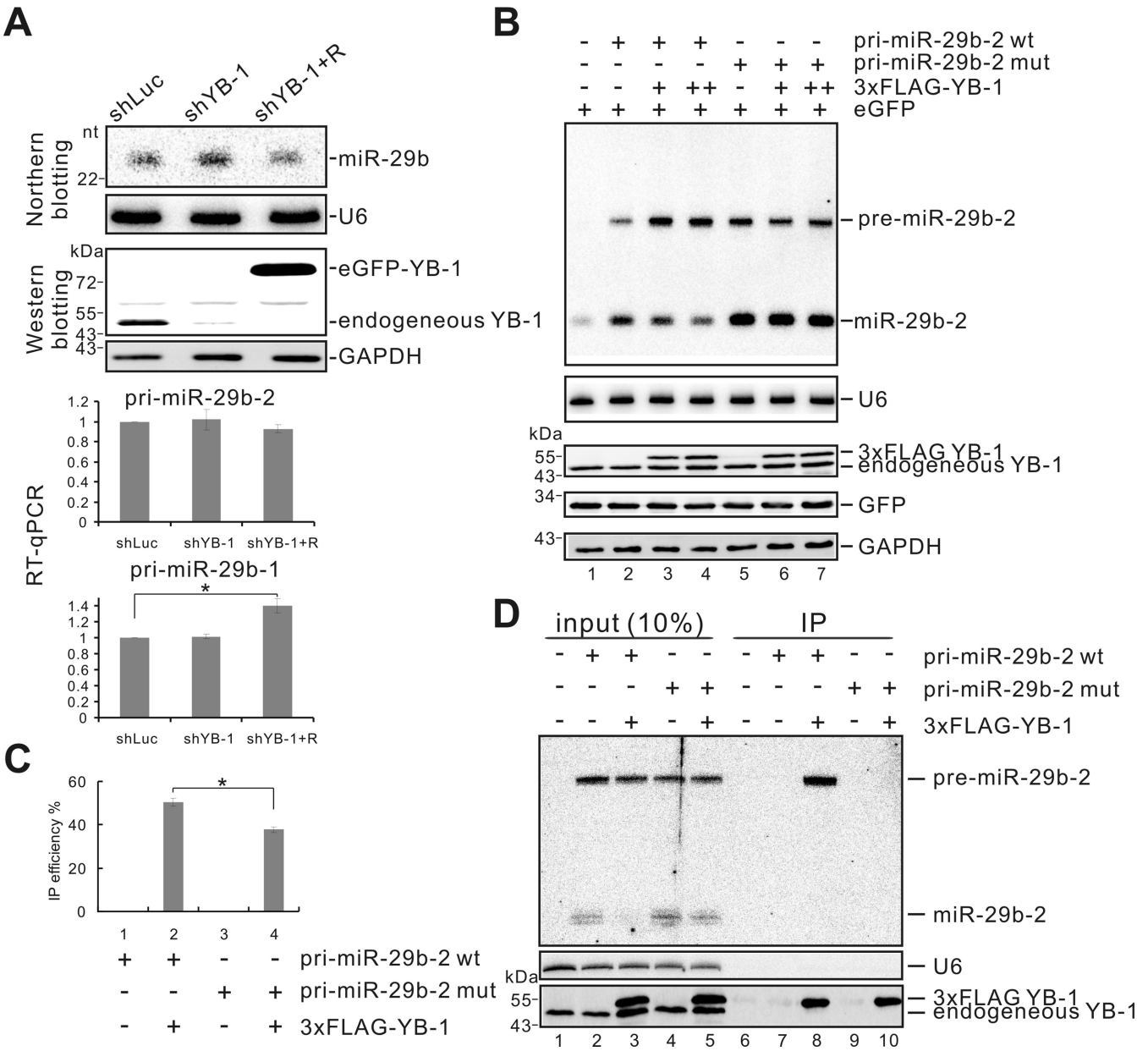

Figure 3. YB-1 suppresses miR-29b-2 biogenesis *in vivo* and associates with pri- and pre-miR-29b-2. (**A**) Northern blotting analysis of the mature miR-29b in cells stably transfected with control (luciferase) shRNA (shLuc), YB-1 shRNA (shYB-1) or co-transfected YB-1 shRNA together with a YB-1-resistant construct (shYB-1+R). The knockdown and rescue effects of YB-1 were determined by Western blotting. U6 and GAPDH served as loading controls. The expression levels of pri-miR-29b-1 and pri-miR-29b-2 were detected by real-time RT-qPCR (*$P < 0.05$, Student's *t*-test). Error bars represent standard deviations ($n = 3$). (**B**) Northern blot analysis of miR-29b-2 in HEK 293T cells co-transfected with 3xFLAG-tagged YB-1 expression construct and the wildtype or the mutant pri-miR-29b-2 plasmid. The GFP expression vector served as a transfection efficiency control. The expression levels of the indicated proteins were detected by western blotting. (**C, D**) RIP analyses of YB-1 bound pri- or pre-miR-29b-2. Immunoprecipitation using anti-FLAG M2 beads was carried out with cell lysate from transfected cells as described in (B). The bound pri-miR-29b-2 and pre-miR-29b-2 were detected by RT-qPCR (**C**) or Northern blotting (**D**), respectively. Error bars represent standard deviations ($n = 3$) in (C) (*$P < 0.05$, Student's *t*-test). The IP efficiency was calculated by Ct values of realtime RT-PCR amplified from the IP-ed samples normalized to the Ct values of input sample. A diagram of the positions of the oligonucleotides used to detect pri-, pre- and mature miR-29b is shown in Supplementary Figure S3.

miR-29b-2 processing at both Drosha and Dicer cleavage steps. To test it, we first prepared the same pri-miR-29b-2 RNAs as in Figure 2C and examined pri-miR-29b-2 processing in HeLa nuclear extract supplemented with recombinant GST or GST-YB-1 fusion protein. GST protein did not affect pri-miR-29b-2 cleavage (Figure 4A, lanes 1–4, 8–11). But the addition of GST-YB-1 inhibited the cleavage of wildtype pri-miR-29b-2 in a dose-dependent manner. In contrast, GST-YB-1 did not affect the cleavage of mutant pri-miR-29b-2 (Figure 4A, lanes 5–7, 12–14). To understand the role of YB-1 binding to the loop of miR-29b-2 in Drosha cleavage, we generated two chimeric pri-miRNA constructs by replacing the terminal loop of pri-miR-24-1 with the wildtype or the mutant loop of miR-29b-2. Re-

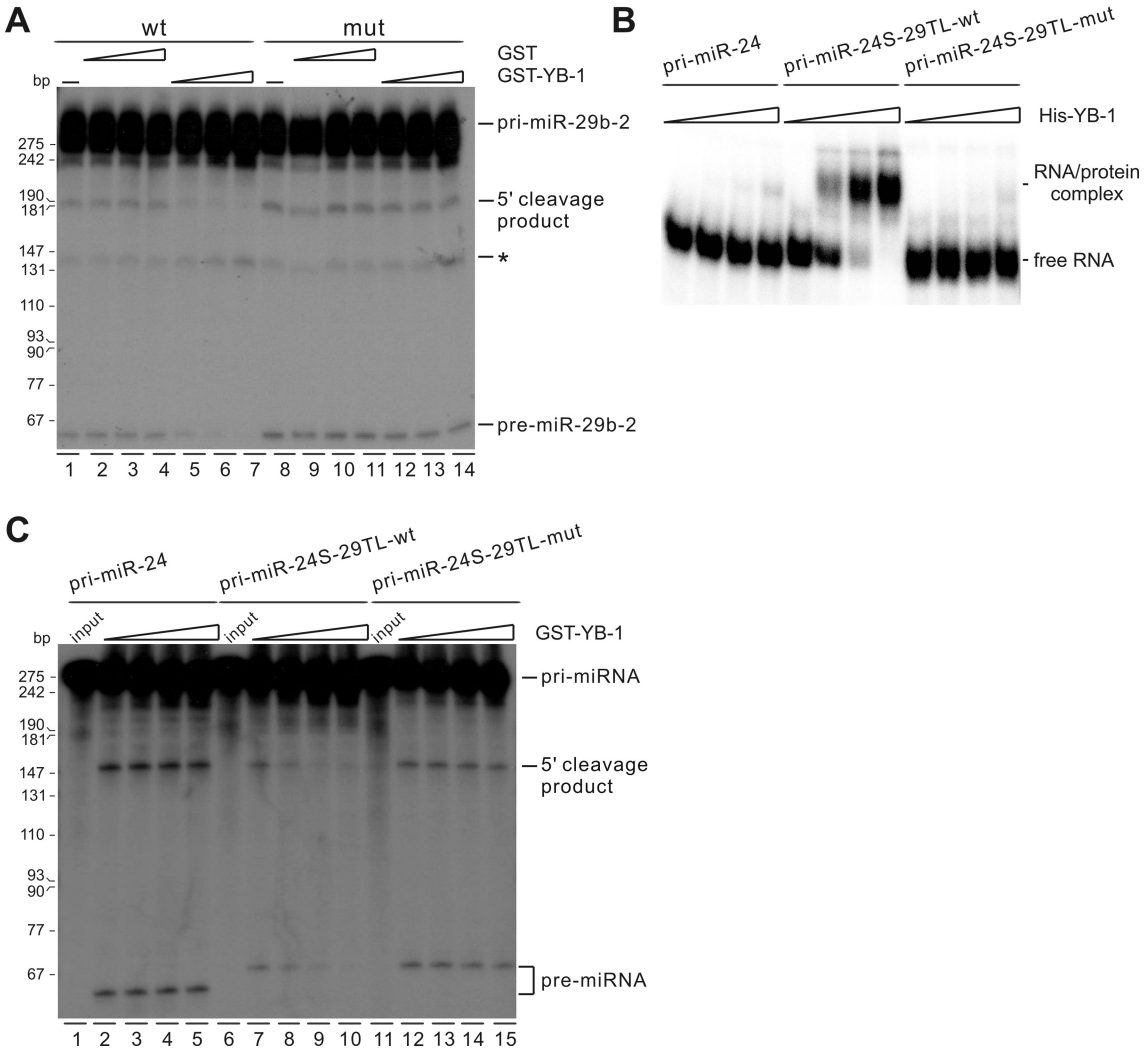

Figure 4. YB-1 inhibits pri-miR-29b-2 processing *in vitro*. (**A, C**) Direct RNA analysis of *in vitro* processing of pri-miR-29b-2. ^{32}P-labeled pri-miR-29b-2 RNAs were incubated with HeLa nuclear extract supplemented with 0, 10, 20 and 40-fold molar excess of GST or GST-YB-1. RNAs were extracted and fractionated on a denaturing polyacrylamide gel. The positions of pri-miR-29b-2, 5′ cleavage product, and pre-miR-29b-2 are indicated on the right. A non-specific cleavage product was labeled with an asterisk. ^{32}P-labeled pcDNA3 HpaII restriction fragments served as size markers. (**B**) Gel shift analysis of His-YB-1 binding to pri-miR-24–1 or its derivatives containing the wildtype or the mutant loop sequence of miR-29b-2 (pri-miR-24S-29TL-wt and pri-miR-24S-29TL-mut).

sults of gel shift assay show that GST-YB-1 only associated with the chimeric pri-miRNA containing the wildtype loop sequence of miR-29b-2 (Figure 4B). In the HeLa nuclear extract, the addition of GST-YB-1 had no influence on the processing of pri-miR-24–1 (Figure 4C, lanes 1–5). However, YB-1 repressed the processing of the chimeric pri-miRNA containing the wildtype loop sequence of miR-29b-2, but not that of the chimeric pri-miRNA carrying the mutant loop of miR-29b-2 (Figure 4C, lanes 6–15). These results indicate that the terminal loop sequence of miR-29b-2 mediates the suppression of Drosha cleavage by YB-1.

We next determined whether YB-1 also inhibits the processing of pre-miR-29b-2 to generate mature miR-29b-2. To this end, ^{32}P-labeled pre-miR-29b-2 produced by ribozyme cleavage was incubated with Dicer purified from transfected cells in the presence of different amounts of recombinant His-YB-1 protein. The addition of His-YB-1 significantly inhibited the processing of wildtype pre-miR-29b-2, but not the mutant one (Figure 5A). Although substitution of the terminal loop sequence of pre-miR-24–1 with that of miR-29b-2 changed Dicer cleavage accuracy, His-YB-1 inhibited all Dicer products processed from the chimeric pre-miRNA containing the wildtype miR-29b-2 loop sequence, but not the mutant loop sequence (Figure 5B). These data demonstrate that YB-1 blocks the maturation of miR-29b-2 at both Drosha and Dicer steps via binding to the terminal loop of miR-29b-2.

YB-1 blocks DGCR8 and Dicer loading to the pri- and pre-miR-29b-2

To gain mechanistic insights into YB-1 mediated-repression of miR-29b-2 maturation, we investigated the effects of YB-1 on the association of DGCR8 with the pri-miR-29b-2 and Dicer with the pre-miR-29b-2, respectively. ^{32}P-labeled

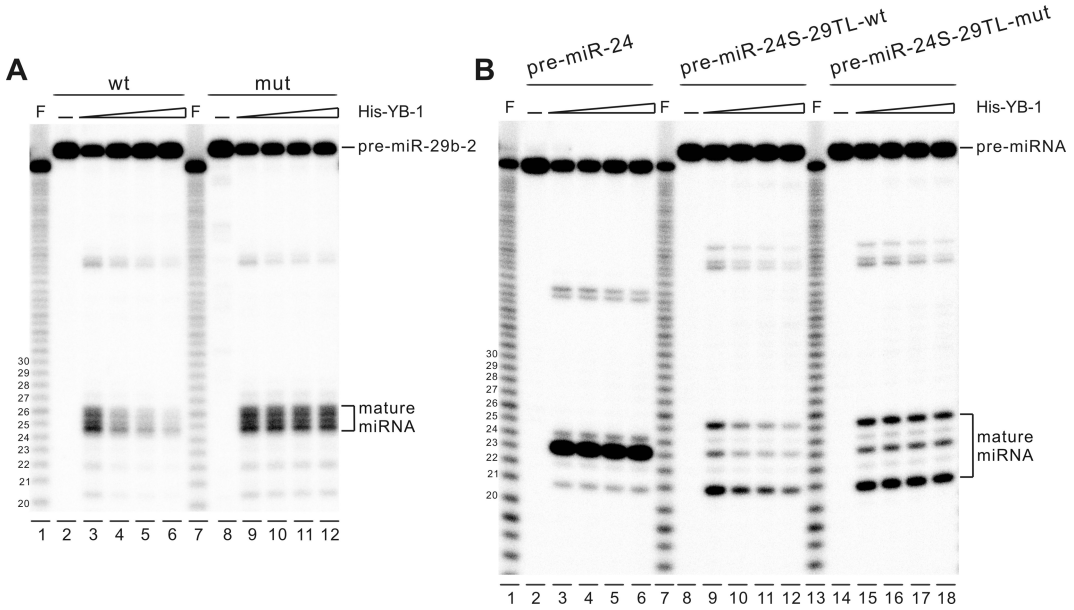

Figure 5. YB-1 blocks the processing of pre-miR-29b-2 *in vitro*. (**A, B**) Direct RNA analyses of *in vitro* processing of pre-miR-29b-2. 5′ end-labeled pre-miR-29b-2, pre-miR-24, and hybrid pre-miR-24-29b-2 RNAs generated by hammerhead ribozyme were incubated with FLAG-tagged Dicer purified from transfected cells in the presence of different amounts of His-YB-1. RNAs were extracted and fractionated on a denaturing polyacrylamide gel. ^{32}P-labeled pre-miR-24 digested with alkaline (F lanes) served as RNA markers. The positions of pre- and mature miRNAs are indicated to the right.

pri-miRNAs were incubated with FLAG-tagged DGCR8 immobilized on anti-FLAG beads. Notably, FLAG-tagged DGCR8 was associated with the pri-miR-29b-2 and the control pri-miR-24–1 RNAs. The addition of His-YB-1 blocked the association between pri-miR-29b-2 and DGCR8 in a dose-dependent manner. In contrast, His-YB-1 did not affect the association between DGCR8 and the pri-miR-24-1 or the mutant pri-miR-29b-2 (Figure 6A). In a similar experiment, we incubated ^{32}P-labeled pre-miR-29b-2 and pre-miR-24–1 with FLAG-tagged Dicer under the condition where Dicer lost its cleavage activity (53). The addition of His-YB-1 inhibited Dicer binding to pre-miR-29b-2 without affecting the binding of Dicer to pre-miR-24-1 or the mutant pre-miR-29b-2 (Figure 6B). We did not detect the association of YB-1 with Drosha/DGCR8 or with Dicer (data not shown). Taken together, these results strongly suggest that YB-1 inhibits miR-29b-2 at Drosha and Dicer cleavage steps by blocking the loading of DGCR8 and Dicer complexes to pri-miR-29b-2 and pre-miR-29b-2, respectively.

The expression levels of YB-1 and miR-29b are inversely correlated in GBM

To determine the significance of the regulation of miR-29b by YB-1, we collected four pairs of normal and tumor tissues as well as 3 tumor samples and analyzed YB-1 expression levels by Western blotting. YB-1 was highly expressed in GBM tissues comparing to adjacent normal tissues (Figure 7A). Interestingly, results of real-time RT-qPCR indicate that the expression levels of miR-29b exhibited an inverse correlation with those of YB-1 (Figure 7B). In three paired tissues in which YB-1 was significantly overexpressed in tumor tissues, compared to normal tissues, miR-29b showed a dramatic reciprocal decrease in expression. Next, we analyzed the expression data of YB-1 and miR-29b obtained from 472 GBM patients in TCGA (The Cancer Genome Atlas) database. A statistically significant but weak inverse correlation was also found between the expression levels of YB-1 and miR-29b expression (Figure 7C).

YB-1 promotes cell proliferation through down-regulation of miR-29b

To investigate whether down-regulation of miR-29b affects tumor cell proliferation, we performed MTT assay in U251-MG cells transfected with miR-29b mimic or antisense oligos. Our results showed that miR-29b mimic inhibited cell growth, while miR-29b antisense oligos promoted cell growth, indicating miR-29b suppresses tumor cell proliferation (Figure 7D). To test whether YB-1 promotes cell proliferation via miR-29b, we next transfected miR-29b antisense oligos into YB-1-knockdown cells. Results of MTT assay showed that knockdown of YB-1 led to a decrease in cell proliferation. Importantly, transfection of miR-29b antisense oligos partially rescued cell growth repression caused by knockdown of YB-1 (Figure 7E). Together, these data indicate that overexpression of YB-1 in GBM promotes cell proliferation partially through down-regulation of miR-29b, a miRNA with tumor suppressor function.

DISCUSSION

In this study, we provide a global view of *in vivo* YB-1–RNA interactions. YB-1 preferentially recognizes a UYAUC sequence motif and binds to the majority of transcribed coding gene transcripts and as well as the stem-loop regions of miRNA precursors. By performing genome-wide analyses

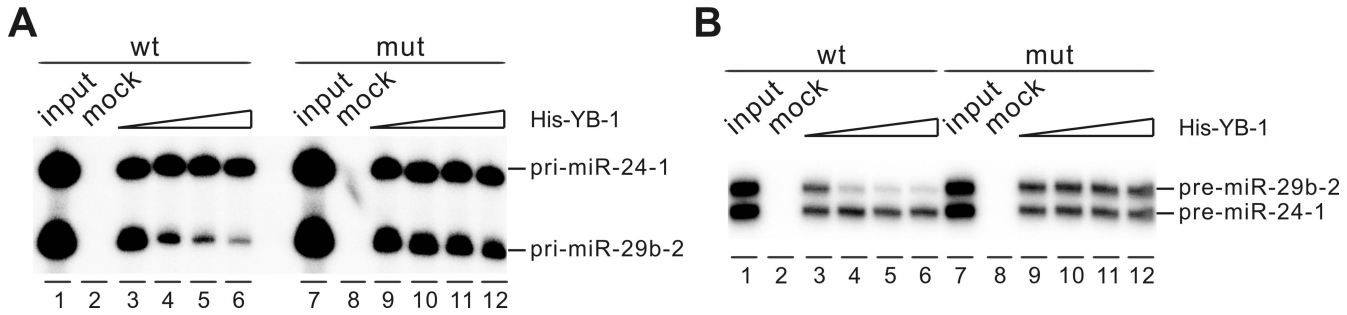

Figure 6. YB-1 competes pri/pre-miRNA with DGCR8 and Dicer. (**A, B**) Pulldown analyses of DGCR8- (**A**) or Dicer- (**B**) bound pri- or pre-miRNAs. FLAG-tagged DGCR8 or Dicer immobilized on beads was incubated with ^{32}P-labeled pri- or pre-miRNAs as indicated in the presence of different amounts of His-YB-1. After extensive washing, the bound RNAs were recovered and separated by a denaturing polyacrylamide gel.

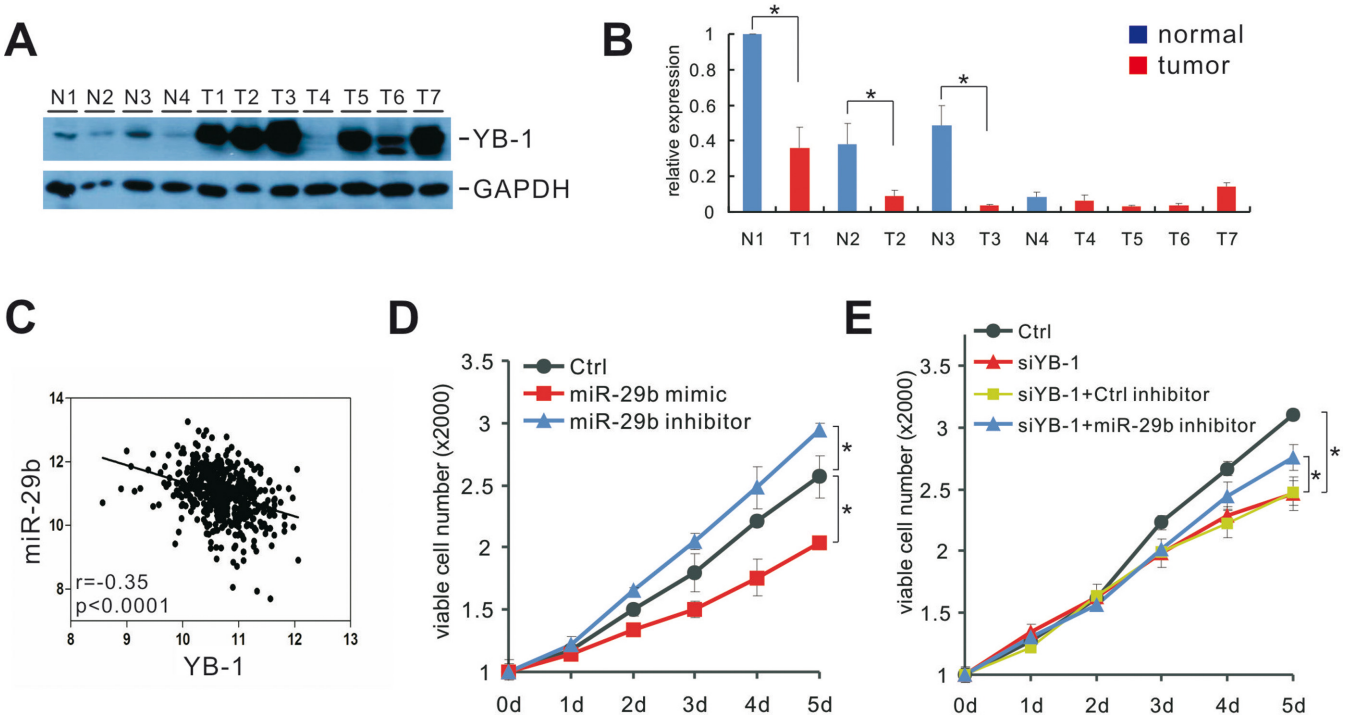

Figure 7. YB-1 regulates cell proliferation in part through miR-29b in GBM. (**A**) Western blot analysis of YB-1 protein levels in GBM tissues (T1–T7) and the adjacent normal tissues of T1–T4 (N1–N4). GAPDH served as a loading control. (**B**) RT-qPCR analysis of miR-29b levels in GBM tissues (T1–T7) and normal tissues (N1–N4). The expression levels of miR-29b in different tissue samples were normalized to that in N1 sample (*$P < 0.05$, Student's *t*-test). Error bars represent standard deviations ($n = 3$). (**C**) Inverse correlation between the expression levels of YB-1 mRNA and miR-29b in 472 GBM patients from TCGA database. (**D**) MTT analysis of cell proliferation in U251-MG cells transfected with control, miR-29b mimic or miR-29b inhibitor, respectively. Error bars represent standard deviations ($n = 3$). (**E**) MTT analysis of cell proliferation in U251-MG cells transfected with control, YB-1 siRNA (siYB-1) or co-transfected with YB-1 siRNA and control- or miR-29b inhibitor, respectively. Error bars represent standard deviations ($n = 3$, *$P < 0.05$, Student's *t*-test).

and biochemical studies, we identified a previously uncharacterized function of YB-1 in the regulation of miRNA processing. Our results indicate that YB-1 promotes cell proliferation through post-transcriptionally repressing the expression of miR-29b, which may be a new marker for GBM.

Glioma is the most common primary brain tumor in children and young adults. A majority of high-grade and malignant gliomas belongs to the type of GBM, which carries a poor prognosis with a median survival of about 15 months (54). A growing body of evidence suggests that altered miRNA expression contributes to GBM development, progression, and metastasis (55,56). However, little is known about the molecular mechanisms that lead to the dysregulation of miRNA expression in GBM. Using iCLIP-seq and small RNA-seq approaches, we identified the oncoprotein YB-1 as a critical regulator of aberrant miRNA expression in GBM. We found that YB-1 up-regulates miR-221/222 through regulating the expression level of their host transcripts (Supplementary Figure S1) and down-regulates miR-29b by inhibiting the biogenesis of miR-29b-2. The miR-221/222 cluster is often overexpressed in GBM and believed to play essential roles in glioma progression (48–51). Intriguingly, our results show that the expression levels of YB-1 and miR-29b are inversely correlated in GBM, and

down-regulation of miR-29b is a new potential biomarker for GBM.

It has long been believed that YB-1 is an abundant mRNA packaging protein and binds to RNA with low sequence specificity. Consistent with the notion that YB-1 is a major component of mRNP, the *in vivo* binding sites of YB-1 detected by iCLIP-seq are enriched in the coding genes. Our iCLIP-seq data also indicate that at least 17.8% of tags carry a UYAUC consensus motif, suggesting that YB-1 binds to a significant fraction of RNA sequences with high sequence specificity. In this study, we provide evidence that through a sequence-specific binding manner, YB-1 interacts with the loop regions of pri- and pre-miR-29b-2 before Drosha and Dicer cleavage and inhibits these two cleavage steps. We also identified YB-1 iCLIP crosslink sites in the loop regions of miR-26a-2, let-7g and let-7a-2, which all contain sequences similar to the YB-1 consensus motif. Overexpression of YB-1 led to a weak inhibitory effect on the maturation of the three miRNAs (data not shown). Considering that much less iCLIP reads were detected in the loop regions of these three miRNAs comparing to miR-29b-2, it implicates that YB-1's inhibitory effect is controlled by the affinity of YB-1 to RNA, which may depend on the cell type and sequence context of target RNA.

Two possible mechanisms exist to explain the novel function of YB-1 in miRNA processing. First, this could be attributed to the RNA-chaperon activity of YB-1 (57). By partially melting of the RNA secondary structure, YB-1 may remodel the pri- or pre-miRNAs into a structure not suitable for cleavage by Drosha and Dicer. Second, YB-1, which can form oligomeric complexes with RNA (58), may block the loading of microprocessor complex or Dicer to the primary or precursor of miR-29b-2 through static hindrance.

Lin28 is a cold shock domain-containing protein that plays important roles in stem cell differentiation and tumorigenesis through regulating let-7 miRNA processing (59,60). Genome-wide CLIP-seq analyses revealed that the Zinc knuckle domain (ZKD) of Lin28 is the major determinant of its RNA binding specificity (61–63). While the CSD of Lin28 binds U-rich sequence, and may remodel the stem loop of pre-let-7 to facilitate the binding of Zinc knuckle to the loop of let-7 or to block the Dicer cleavage site (64–66). By comparing the protein sequences between YB-1 and Lin28, we found that the RNP-1 and RNP-2 motifs are identical between these two proteins, but Lin28 contains an extra 9 aa linker sequence between RNP-1 and RNP-2. It is possible that the different size of linker sequence and the flanking domains lead to distinct RNA binding specificity and affinity between YB-1 and Lin28. It has been previously reported that YB-1 knockout mice result in embryonic lethality (67,68). In the future, it is interesting to test whether YB-1-mediated miRNA processing regulation also plays a role in embryonic development. Taken together, our findings establish a new pathway in the control of tumor cell proliferation involving YB-1 mediated-dysregulation of miR-29b expression and reveal a new function of YB-1 in the regulation of miRNA processing in GBM.

AVAILABILITY

The iCLIP data containing information for YB-1 crosslink sites and cDNA counts are available on the website www.sibcb.ac.cn/hui.asp.

SUPPLEMENTARY DATA

Supplementary Data are available at NAR Online.

ACKNOWLEDGEMENTS

We thank Narry Kim, Sandra E. Dunn, and Kimitoshi Kohno for providing plasmids, Jun Zhu for helping with small RNA-seq data analysis, Ying Huang for valuable discussion, and Zhongsheng You for critical reading of the manuscript.

FUNDING

National Basic Research Program of China [2011CBA01105, 2011CB811304] and National Natural Science Foundation of China [31370787] to Jingyi Hui; Eastern Scholar from the Shanghai Institutions of Higher Learning [QD2015005] and Shanghai Pujiang Program from the Science and Technology Commission of Shanghai Municipality [15PJ140530] to Jinyan Huang. Funding for open access charge: National Basic Research Program of China [2011CBA01105, 2011CB811304] and National Natural Science Foundation of China [31370787] to J.H.
Conflict of interest statement. None declared.

REFERENCES

1. Bartel,D.P. (2009) MicroRNAs: target recognition and regulatory functions. *Cell*, **136**, 215–233.
2. Lee,Y., Ahn,C., Han,J., Choi,H., Kim,J., Yim,J., Lee,J., Provost,P., Radmark,O., Kim,S. *et al.* (2003) The nuclear RNase III Drosha initiates microRNA processing. *Nature*, **425**, 415–419.
3. Han,J., Lee,Y., Yeom,K.H., Kim,Y.K., Jin,H. and Kim,V.N. (2004) The Drosha-DGCR8 complex in primary microRNA processing. *Genes Dev.*, **18**, 3016–3027.
4. Landthaler,M., Yalcin,A. and Tuschl,T. (2004) The human DiGeorge syndrome critical region gene 8 and Its D. melanogaster homolog are required for miRNA biogenesis. *Curr. Biol.*, **14**, 2162–2167.
5. Lee,Y., Kim,M., Han,J., Yeom,K.H., Lee,S., Baek,S.H. and Kim,V.N. (2004) MicroRNA genes are transcribed by RNA polymerase II. *EMBO J.*, **23**, 4051–4060.
6. Yi,R., Qin,Y., Macara,I.G. and Cullen,B.R. (2003) Exportin-5 mediates the nuclear export of pre-microRNAs and short hairpin RNAs. *Genes Dev.*, **17**, 3011–3016.
7. Bernstein,E., Caudy,A.A., Hammond,S.M. and Hannon,G.J. (2001) Role for a bidentate ribonuclease in the initiation step of RNA interference. *Nature*, **409**, 363–366.
8. Hammond,S.M., Boettcher,S., Caudy,A.A., Kobayashi,R. and Hannon,G.J. (2001) Argonaute2, a link between genetic and biochemical analyses of RNAi. *Science*, **293**, 1146–1150.
9. Farazi,T.A., Hoell,J.I., Morozov,P. and Tuschl,T. (2013) MicroRNAs in human cancer. *Adv. Exp. Med. Biol.*, **774**, 1–20.
10. Guil,S. and Caceres,J.F. (2007) The multifunctional RNA-binding protein hnRNP A1 is required for processing of miR-18a. *Nat. Struct. Mol. Biol.*, **14**, 591–596.
11. Kim,K.K., Yang,Y., Zhu,J., Adelstein,R.S. and Kawamoto,S. (2014) Rbfox3 controls the biogenesis of a subset of microRNAs. *Nat. Struct. Mol. Biol.*, **21**, 901–910.
12. Trabucchi,M., Briata,P., Garcia-Mayoral,M., Haase,A.D., Filipowicz,W., Ramos,A., Gherzi,R. and Rosenfeld,M.G. (2009) The RNA-binding protein KSRP promotes the biogenesis of a subset of microRNAs. *Nature*, **459**, 1010–1014.

13. Viswanathan,S.R., Daley,G.Q. and Gregory,R.I. (2008) Selective blockade of microRNA processing by Lin28. *Science*, **320**, 97–100.
14. Wu,H., Sun,S., Tu,K., Gao,Y., Xie,B., Krainer,A.R. and Zhu,J. (2010) A splicing-independent function of SF2/ASF in microRNA processing. *Mol. Cell*, **38**, 67–77.
15. Han,C., Liu,Y., Wan,G., Choi,H.J., Zhao,L., Ivan,C., He,X., Sood,A.K., Zhang,X. and Lu,X. (2014) The RNA-binding protein DDX1 promotes primary microRNA maturation and inhibits ovarian tumor progression. *Cell Rep.*, **8**, 1447–1460.
16. Eliseeva,I.A., Kim,E.R., Guryanov,S.G., Ovchinnikov,L.P. and Lyabin,D.N. (2011) Y-box-binding protein 1 (YB-1) and its functions. *Biochemistry (Mosc.)*, **76**, 1402–1433.
17. Lyabin,D.N., Eliseeva,I.A. and Ovchinnikov,L.P. (2014) YB-1 protein: functions and regulation. *Wiley Interdiscip. Rev. RNA*, **5**, 95–110.
18. Lasham,A., Print,C.G., Woolley,A.G., Dunn,S.E. and Braithwaite,A.W. (2013) YB-1: oncoprotein, prognostic marker and therapeutic target? *Biochem J.*, **449**, 11–23.
19. Kosnopfel,C., Sinnberg,T. and Schittek,B. (2014) Y-box binding protein 1–a prognostic marker and target in tumour therapy. *Eur. J. Cell Biol.*, **93**, 61–70.
20. Bergmann,S., Royer-Pokora,B., Fietze,E., Jurchott,K., Hildebrandt,B., Trost,D., Leenders,F., Claude,J.C., Theuring,F., Bargou,R. *et al.* (2005) YB-1 provokes breast cancer through the induction of chromosomal instability that emerges from mitotic failure and centrosome amplification. *Cancer Res.*, **65**, 4078–4087.
21. Bargou,R.C., Jurchott,K., Wagener,C., Bergmann,S., Metzner,S., Bommert,K., Mapara,M.Y., Winzer,K.J., Dietel,M., Dorken,B. *et al.* (1997) Nuclear localization and increased levels of transcription factor YB-1 in primary human breast cancers are associated with intrinsic MDR1 gene expression. *Nat. Med.*, **3**, 447–450.
22. En-Nia,A., Yilmaz,E., Klinge,U., Lovett,D.H., Stefanidis,I. and Mertens,P.R. (2005) Transcription factor YB-1 mediates DNA polymerase alpha gene expression. *J. Biol. Chem.*, **280**, 7702–7711.
23. Wu,J., Lee,C., Yokom,D., Jiang,H., Cheang,M.C., Yorida,E., Turbin,D., Berquin,I.M., Mertens,P.R., Iftner,T. *et al.* (2006) Disruption of the Y-box binding protein-1 results in suppression of the epidermal growth factor receptor and HER-2. *Cancer Res.*, **66**, 4872–4879.
24. Finkbeiner,M.R., Astanehe,A., To,K., Fotovati,A., Davies,A.H., Zhao,Y., Jiang,H., Stratford,A.L., Shadeo,A., Boccaccio,C. *et al.* (2009) Profiling YB-1 target genes uncovers a new mechanism for MET receptor regulation in normal and malignant human mammary cells. *Oncogene*, **28**, 1421–1431.
25. Evdokimova,V., Tognon,C., Ng,T., Ruzanov,P., Melnyk,N., Fink,D., Sorokin,A., Ovchinnikov,L.P., Davicioni,E., Triche,T.J. *et al.* (2009) Translational activation of snail1 and other developmentally regulated transcription factors by YB-1 promotes an epithelial-mesenchymal transition. *Cancer Cell*, **15**, 402–415.
26. El-Naggar,A.M., Veinotte,C.J., Cheng,H., Grunewald,T.G., Negri,G.L., Somasekharan,S.P., Corkery,D.P., Tirode,F., Mathers,J., Khan,D. *et al.* (2015) Translational Activation of HIF1alpha by YB-1 Promotes Sarcoma Metastasis. *Cancer Cell*, **27**, 682–697.
27. Bouvet,P., Matsumoto,K. and Wolffe,A.P. (1995) Sequence-specific RNA recognition by the Xenopus Y-box proteins. An essential role for the cold shock domain. *J. Biol. Chem.*, **270**, 28297–28303.
28. Matsumoto,K., Meric,F. and Wolffe,A.P. (1996) Translational repression dependent on the interaction of the Xenopus Y-box protein FRGY2 with mRNA. Role of the cold shock domain, tail domain, and selective RNA sequence recognition. *J. Biol. Chem.*, **271**, 22706–22712.
29. Manival,X., Ghisolfi-Nieto,L., Joseph,G., Bouvet,P. and Erard,M. (2001) RNA-binding strategies common to cold-shock domain- and RNA recognition motif-containing proteins. *Nucleic Acids Res.*, **29**, 2223–2233.
30. Ise,T., Nagatani,G., Imamura,T., Kato,K., Takano,H., Nomoto,M., Izumi,H., Ohmori,H., Okamoto,T., Ohga,T. *et al.* (1999) Transcription factor Y-box binding protein 1 binds preferentially to cisplatin-modified DNA and interacts with proliferating cell nuclear antigen. *Cancer Res.*, **59**, 342–346.
31. Okamoto,T., Izumi,H., Imamura,T., Takano,H., Ise,T., Uchiumi,T., Kuwano,M. and Kohno,K. (2000) Direct interaction of p53 with the Y-box binding protein, YB-1: a mechanism for regulation of human gene expression. *Oncogene*, **19**, 6194–6202.
32. Wei,W.J., Mu,S.R., Heiner,M., Fu,X., Cao,L.J., Gong,X.F., Bindereif,A. and Hui,J. (2012) YB-1 binds to CAUC motifs and stimulates exon inclusion by enhancing the recruitment of U2AF to weak polypyrimidine tracts. *Nucleic Acids Res.*, **40**, 8622–8636.
33. Minich,W.B., Maidebura,I.P. and Ovchinnikov,L.P. (1993) Purification and characterization of the major 50-kDa repressor protein from cytoplasmic mRNP of rabbit reticulocytes. *Eur. J. Biochem.*, **212**, 633–638.
34. Evdokimova,V.M., Wei,C.L., Sitikov,A.S., Simonenko,P.N., Lazarev,O.A., Vasilenko,K.S., Ustinov,V.A., Hershey,J.W. and Ovchinnikov,L.P. (1995) The major protein of messenger ribonucleoprotein particles in somatic cells is a member of the Y-box binding transcription factor family. *J. Biol. Chem.*, **270**, 3186–3192.
35. Stickeler,E., Fraser,S.D., Honig,A., Chen,A.L., Berget,S.M. and Cooper,T.A. (2001) The RNA binding protein YB-1 binds A/C-rich exon enhancers and stimulates splicing of the CD44 alternative exon v4. *EMBO J.*, **20**, 3821–3830.
36. Skabkina,O.V., Lyabin,D.N., Skabkin,M.A. and Ovchinnikov,L.P. (2005) YB-1 autoregulates translation of its own mRNA at or prior to the step of 40S ribosomal subunit joining. *Mol. Cell. Biol.*, **25**, 3317–3323.
37. Konig,J., Zarnack,K., Rot,G., Curk,T., Kayikci,M., Zupan,B., Turner,D.J., Luscombe,N.M. and Ule,J. (2010) iCLIP reveals the function of hnRNP particles in splicing at individual nucleotide resolution. *Nat. Struct. Mol. Biol.*, **17**, 909–915.
38. Langmead,B., Trapnell,C., Pop,M. and Salzberg,S.L. (2009) Ultrafast and memory-efficient alignment of short DNA sequences to the human genome. *Genome Biol.*, **10**, R25.
39. Rossbach,O., Hung,L.H., Khrameeva,E., Schreiner,S., Konig,J., Curk,T., Zupan,B., Ule,J., Gelfand,M.S. and Bindereif,A. (2014) Crosslinking-immunoprecipitation (iCLIP) analysis reveals global regulatory roles of hnRNP L. *RNA Biol.*, **11**, 146–155.
40. Martin,M. (2011) Cutadapt removes adapter sequences from high-throughput sequencing reads. *EMBnet.journal*, **17**, 10–12.
41. Quinlan,A.R. and Hall,I.M. (2010) BEDTools: a flexible suite of utilities for comparing genomic features. *Bioinformatics*, **26**, 841–842.
42. Kozomara,A. and Griffiths-Jones,S. (2014) miRBase: annotating high confidence microRNAs using deep sequencing data. *Nucleic Acids Res.*, **42**, D68–D73.
43. Zong,F.Y., Fu,X., Wei,W.J., Luo,Y.G., Heiner,M., Cao,L.J., Fang,Z., Fang,R., Lu,D., Ji,H. *et al.* (2014) The RNA-binding protein QKI suppresses cancer-associated aberrant splicing. *PLoS Genet.*, **10**, e1004289.
44. Chen,C., Ridzon,D.A., Broomer,A.J., Zhou,Z., Lee,D.H., Nguyen,J.T., Barbisin,M., Xu,N.L., Mahuvakar,V.R., Andersen,M.R. *et al.* (2005) Real-time quantification of microRNAs by stem-loop RT-PCR. *Nucleic Acids Res.*, **33**, e179.
45. Ferre-D'Amare,A.R. and Doudna,J.A. (1996) Use of cis- and trans-ribozymes to remove 5′ and 3′ heterogeneities from milligrams of in vitro transcribed RNA. *Nucleic Acids Res.*, **24**, 977–978.
46. Cancer Genome Atlas Research, N. (2008) Comprehensive genomic characterization defines human glioblastoma genes and core pathways. *Nature*, **455**, 1061–1068.
47. Cazalla,D., Xie,M. and Steitz,J.A. (2011) A primate herpesvirus uses the integrator complex to generate viral microRNAs. *Mol. Cell*, **43**, 982–992.
48. Gillies,J.K. and Lorimer,I.A. (2007) Regulation of p27Kip1 by miRNA 221/222 in glioblastoma. *Cell Cycle*, **6**, 2005–2009.
49. Medina,R., Zaidi,S.K., Liu,C.G., Stein,J.L., van Wijnen,A.J., Croce,C.M. and Stein,G.S. (2008) MicroRNAs 221 and 222 bypass quiescence and compromise cell survival. *Cancer Res.*, **68**, 2773–2780.
50. Quintavalle,C., Garofalo,M., Zanca,C., Romano,G., Iaboni,M., del Basso De Caro,M., Martinez-Montero,J.C., Incoronato,M., Nuovo,G., Croce,C.M. *et al.* (2012) miR-221/222 overexpression in human glioblastoma increases invasiveness by targeting the protein phosphate PTPmu. *Oncogene*, **31**, 858–868.
51. Zhang,J., Han,L., Ge,Y., Zhou,X., Zhang,A., Zhang,C., Zhong,Y., You,Y., Pu,P. and Kang,C. (2010) miR-221/222 promote malignant progression of glioma through activation of the Akt pathway. *Int. J. Oncol.*, **36**, 913–920.
52. Chang,T.C., Yu,D., Lee,Y.S., Wentzel,E.A., Arking,D.E., West,K.M., Dang,C.V., Thomas-Tikhonenko,A. and Mendell,J.T. (2008) Widespread microRNA repression by Myc contributes to tumorigenesis. *Nat. Genet.*, **40**, 43–50.

53. Zhang,H., Kolb,F.A., Brondani,V., Billy,E. and Filipowicz,W. (2002) Human Dicer preferentially cleaves dsRNAs at their termini without a requirement for ATP. *EMBO J.*, **21**, 5875–5885.
54. Furnari,F.B., Fenton,T., Bachoo,R.M., Mukasa,A., Stommel,J.M., Stegh,A., Hahn,W.C., Ligon,K.L., Louis,D.N., Brennan,C. *et al.* (2007) Malignant astrocytic glioma: genetics, biology, and paths to treatment. *Genes Dev.*, **21**, 2683–2710.
55. Karsy,M., Arslan,E. and Moy,F. (2012) Current Progress on Understanding MicroRNAs in Glioblastoma Multiforme. *Genes Cancer*, **3**, 3–15.
56. Brower,J.V., Clark,P.A., Lyon,W. and Kuo,J.S. (2014) MicroRNAs in cancer: glioblastoma and glioblastoma cancer stem cells. *Neurochem Int*, **77**, 68–77.
57. Skabkin,M.A., Evdokimova,V., Thomas,A.A. and Ovchinnikov,L.P. (2001) The major messenger ribonucleoprotein particle protein p50 (YB-1) promotes nucleic acid strand annealing. *J. Biol. Chem.*, **276**, 44841–44847.
58. Skabkin,M.A., Kiselyova,O.I., Chernov,K.G., Sorokin,A.V., Dubrovin,E.V., Yaminsky,I.V., Vasiliev,V.D. and Ovchinnikov,L.P. (2004) Structural organization of mRNA complexes with major core mRNP protein YB-1. *Nucleic Acids Res.*, **32**, 5621–5635.
59. West,J.A., Viswanathan,S.R., Yabuuchi,A., Cunniff,K., Takeuchi,A., Park,I.H., Sero,J.E., Zhu,H., Perez-Atayde,A., Frazier,A.L. *et al.* (2009) A role for Lin28 in primordial germ-cell development and germ-cell malignancy. *Nature*, **460**, 909–913.
60. Piskounova,E., Polytarchou,C., Thornton,J.E., LaPierre,R.J., Pothoulakis,C., Hagan,J.P., Iliopoulos,D. and Gregory,R.I. (2011) Lin28A and Lin28B inhibit let-7 microRNA biogenesis by distinct mechanisms. *Cell*, **147**, 1066–1079.
61. Cho,J., Chang,H., Kwon,S.C., Kim,B., Kim,Y., Choe,J., Ha,M., Kim,Y.K. and Kim,V.N. (2012) LIN28A is a suppressor of ER-associated translation in embryonic stem cells. *Cell*, **151**, 765–777.
62. Graf,R., Munschauer,M., Mastrobuoni,G., Mayr,F., Heinemann,U., Kempa,S., Rajewsky,N. and Landthaler,M. (2013) Identification of LIN28B-bound mRNAs reveals features of target recognition and regulation. *RNA Biol.*, **10**, 1146–1159.
63. Wilbert,M.L., Huelga,S.C., Kapeli,K., Stark,T.J., Liang,T.Y., Chen,S.X., Yan,B.Y., Nathanson,J.L., Hutt,K.R., Lovci,M.T. *et al.* (2012) LIN28 binds messenger RNAs at GGAGA motifs and regulates splicing factor abundance. *Mol. Cell*, **48**, 195–206.
64. Nam,Y., Chen,C., Gregory,R.I., Chou,J.J. and Sliz,P. (2011) Molecular Basis for Interaction of let-7 MicroRNAs with Lin28. *Cell*, **147**, 1080–1091.
65. Mayr,F., Schutz,A., Doge,N. and Heinemann,U. (2012) The Lin28 cold-shock domain remodels pre-let-7 microRNA. *Nucleic Acids Res.*, **40**, 7492–7506.
66. Lightfoot,H.L., Bugaut,A., Armisen,J., Lehrbach,N.J., Miska,E.A. and Balasubramanian,S. (2011) A LIN28-dependent structural change in pre-let-7g directly inhibits Dicer processing. *Biochemistry*, **50**, 7514–7521.
67. Lu,Z.H., Books,J.T. and Ley,T.J. (2005) YB-1 is important for late-stage embryonic development, optimal cellular stress responses, and the prevention of premature senescence. *Mol. Cell. Biol.*, **25**, 4625–4637.
68. Uchiumi,T., Fotovati,A., Sasaguri,T., Shibahara,K., Shimada,T., Fukuda,T., Nakamura,T., Izumi,H., Tsuzuki,T., Kuwano,M. *et al.* (2006) YB-1 is important for an early stage embryonic development: neural tube formation and cell proliferation. *J. Biol. Chem.*, **281**, 40440–40449.